THE IONIZING RADIATION FIELD OF NGC 4388 AND ITS RELATION TO THE EXTRANUCLEAR EMISSION-LINE REGIONS[1]

LUIS COLINA
Space Telescope Science Institute, Baltimore, MD 21218 and Departamento Física Teórica, Universidad Autónoma, Madrid, Spain
Received 1990 November 21; accepted 1991 August 2

ABSTRACT

New long-slit spectroscopic observations of NGC 4388 and the extranuclear emission line regions around it are used to investigate the characteristics of the ionizing source and the structure of the extended emission-line regions.

The measured luminosity of the [Fe VII] $\lambda6087$ emission line detected in the nucleus of NGC 4388 is interpreted as evidence for the existence of a powerful ionizing source with $N_{ph}(\geq 100 \text{ eV}) \gtrsim 2 \times 10^{50}$ photons s^{-1} and for the presence of clouds of gas with electron densities $N_e \approx 10^7 \text{ cm}^{-3}$.

A comparison between the far-infrared luminosity and the UV-extrapolated ionizing luminosity as measured along our line of sight suggests that NGC 4388 has a hidden UV luminous source in its nucleus which is around 6 times brighter than observed; it should therefore be obscured by $A_V = 0.31$ mag. This places NGC 4388 among the intermediate luminosity Seyfert 1 galaxies with $\log L_{UV} \approx 43.23$ ergs s^{-1} and confirm the suggestion by Shields and Filippenko that NGC 4388 has a hidden luminous Seyfert 1 nucleus.

The excitation conditions in the extranuclear emission-line regions are best accounted for by the ionization from a nonthermal central source in the nucleus of NGC 4388. Other alternative ionization sources, like star clusters or relativistic particles and shocks associated with the radio emission, are seen to play a minor role, if any.

Subject headings: galaxies: individual (NGC 4388) — galaxies: nuclei — galaxies: Seyfert

1. INTRODUCTION

The questions of whether or not the radiation field of the nuclei of active galaxies is emitted isotropically, and whether or not all Seyfert 2 galaxies are obscured Seyfert 1 galaxies, have been the topic of many investigations over the past few years. Extended high-excitation emission-line regions have been used to detect and constrain the presence of hidden active nuclei in galaxies. An ideal candidate to investigate these questions is the Seyfert galaxy NGC 4388, a galaxy which is known to contain high-excitation extranuclear extended emission-line regions, a broad Hα emission-line profile off the nucleus and an elongated radio structure.

Much evidence has accumulated over the past few years showing that all types of active galaxies could somehow radiate anisotropically (obscuration/beaming/accretion disk), and therefore suggesting that much of the diversity displayed by AGNs is simply a matter of different viewing angles (see Browne 1989 for a review).

The idea that hidden, luminous, active nuclei are common among Seyfert 2 galaxies received strong support with the detection of wide UV ionizing cones in a number of nearby galaxies (Pogge 1988; Tadhunter & Tzvetanov 1989; Pérez et al. 1989; Pérez-Fournon & Wilson 1990; Colina, Sparks, & Macchetto 1991). Also, alignments between radio structure and extended emission-line regions have been detected both at low redshift (Unger et al. 1987; Wilson, Ward, & Haniff 1988; Wilson & Baldwin 1989; Macchetto et al. 1990) and high redshift (Chambers, Miley, & van Breugel 1987; McCarthy et al. 1987). Finally the unification of radio loud quasars and radio

galaxies has been proposed under the hypothesis that a narrow radiation beam is viewed from different angles (Barthel 1989).

On the theoretical side, there are a number of models which predict an angular dependence of the radiation field of a thick accretion disk around a central black hole (Netzer 1985; Madau 1988; Acosta-Pulido et al. 1990).

NGC 4388 is a highly inclined spiral galaxy ($i = 75°$, Hummel et al. 1983) located at the core of the Virgo cluster (Phillips & Malin 1982, hereinafter PM). Throughout this paper NGC 4388 will be considered to be at a distance of 19.7 Mpc (Sandage & Tammann 1984).

Based on its optical emission-line spectrum, PM classified NGC 4388 as a galaxy with a Seyfert type 2 nucleus. However, Filippenko & Sargent (1985) detected broad Hα emission in the nucleus of NGC 4388, indicating faint Seyfert 1 activity. Ultraviolet observations with *IUE* (Ferland & Osterbrock 1986) show a blue continuum source concentrated within the inner 2″ around the nucleus. *Einstein* X-ray observations (Forman et al. 1979) detected NGC 4388 as the fourth strongest X-ray source in the Virgo cluster with a luminosity log $L_x(0.5–3.0 \text{ keV}) = 40.23$ ergs s^{-1}, while very recent hard X-ray observations with the University of Birmingham X-ray telescope detected NGC 4388 as the strongest Virgo cluster source with a measured luminosity log $L_x(2–10 \text{ keV}) = 42.0$ ergs s^{-1} (Hanson et al. 1990).

High-resolution optical spectroscopy showed the presence of a peculiar red asymmetric profile in the [O III] emission lines (Heckman et al. 1983). This was interpreted as combination of independent gas clouds with different physical and kinematic conditions (Colina et al. 1987). More recently, Shields & Filippenko (1988) discovered a faint, broad Hα component (FWHM $\approx 4000 \text{ km s}^{-1}$) off the nucleus and interpreted it as dust-scattered radiation from an obscured Seyfert 1 nucleus. Pogge (1988) detected the presence of high-excitation extra-

---

nuclear extended emission-line regions above the galactic plane of NGC 4388, drawing a conelike geometry, while Corbin, Baldwin, & Wilson (1988) measured velocities in some of these high-excitation gas clouds significantly discrepant from the velocity field of the galaxy. They interpreted this result as evidence for gas ejected from the main body of NGC 4388.

NGC 4388 has also been detected as an *IRAS* source with a total far-infrared luminosity log $L_{\mathrm{FIR}} = 43.43$ ergs s^{-1}. Early radio observations (Hummel, van Gorkom, & Kotanyi 1983) showed a structure composed of a disk with an extension above and perpendicular to the disk itself. New VLA observations of the nucleus detected a tongue of radio emission around position angle (P.A. 20°) as well as two emission peaks separated by 2″ (Stone, Wilson, & Ward 1988; Saikia & Hummel 1989) and close to (but not coincident with) the optical nucleus (Stone et al. 1988). This displacement between the radio and optical nuclei suggests that the true nucleus could be obscured.

All these characteristics make NGC 4388 a good candidate to further investigate the hypothesis of Seyfert 2 galaxies being obscured Seyfert 1 galaxies together with the idea of anisotropy in the radiation field of AGNs.

In this paper we present new low-resolution long-slit spectra along the radio emission axis (P.A. 23°) and the extended emission-line regions (P.A. 35° and P.A. 55°). These spectra are used to constrain the physical conditions (temperature, density, mass, excitation) within the emission-line clouds and to discuss the substructure of the extended emission-line regions, the source of ionization, its properties, and its relation to the source of the radio emission.

2. OBSERVATIONS AND REDUCTIONS

Long-slit spectroscopic observations were done in 1989 February at the German-Spanish observatory in Calar Alto, Spain. The spectra were obtained at three different orientations along position angles 23°, 35°, and 55°. These correspond to the previously known directions where the radio emission and extranuclear emission-like regions are located.

The spectrograph was attached to the Cassegrain focus of the 3.5 m telescope giving a spectral dispersion of 240 Å mm^{-1} and a slit width of 2″ projected onto the sky. The detector was an RCA CCD camera of 512 × 320 pixels of 30 μm each, covering the spectral range between 4000 and 7600 Å and giving a projected size on the sky of 1″15 pixel^{-1}. This setup gives an effective resolution of around 12 Å (FWHM). The exposure time was 20 minutes per position angle, and the seeing had a steady value of 2″5 at FWHM. To avoid differential refraction effects, all observations were done with the telescope pointing near the zenith.

Feige 25 and HZ 44 were used as standard stars observed through a slit width of 6″ to get the detector spectral response. The reduction procedure, following the standard steps, was done using the IRAF software package installed at STScI.

In order to get an idea of the accuracy of our spectroscopy a comparison between our measured emission-line intensity ratios for the nucleus of NGC 4388 and those obtained by PM and Pogge (1988) through comparable apertures is given in Table 1. Our results represent the mean of three independent measurements at P.A. 23°, 35°, and 55°, centered on the peak emission and over a region of 2″ × 3″5, and the error indicates the deviation from the mean value. Errors in the line ratios measured by Pogge (1988) are of the order of 15% except for weak lines where larger errors are expected (Pogge 1988). The

TABLE 1
EMISSION-LINE RATIOS OF THE NUCLEUS OF NGC 4388

Line	Phillips & Malin[a]	Pogge[b]	This work[c]
Hγ	0.36	...	0.45 ± 0.06
[O III] λ4363	0.13	0.20	0.20 ± 0.05
He II λ4686	0.20	0.20	0.21 ± 0.01
Hβ	1.00	1.00	1.00
[O III] λ5007	11.20	10.30	11.71 ± 0.15
[O I] λ6300	0.78	0.85	0.76 ± 0.13
[N II] λ6548	0.86	1.14	0.75 ± 0.09
Hα	4.86	5.14	4.55 ± 0.72
[N II] λ6584	2.59	3.42	2.61 ± 0.34
[S II] λ6717	1.27	1.60	1.39 ± 0.08
[S II] λ6731	1.12	1.61	1.31 ± 0.22

[a] Line ratios from Phillips & Malin 1982 through an aperture of 2″ × 4″.
[b] Line ratios of the nucleus from Table 1 in Pogge 1988.
[c] Mean of the values obtained at P.A. 23°, 35°, and 55°.

accuracy of the PM measurements is between 10% and 20%. Within these uncertainties, our results are in agreement with both previous observations.

Since intermittent cirrus clouds were present, we also checked the absolute flux calibration against the values given by PM. More precisely, a comparison was done between the mean flux measured for the [O III] λ5007 emission line around the nucleus (2″ × 3″5) at the three different position angles observed and the reported value by PM for an aperture of 2″ × 4″ centered on the optical nucleus. Our mean value, $F([O III] \lambda5007) = 1.86 \pm 1.26 \times 10^{-13}$ ergs cm^{-2} s^{-1}, agrees well with that of PM: $F([O III] \lambda5007) = 1.83 \times 10^{-13}$ ergs cm^{-2} s^{-1}. However, our uncertainty in the absolute flux is large, and therefore the quoted line luminosities should be considered valid to within a factor of 2.

3. RESULTS

3.1. *Extinction and Amount of Dust within the Emission-Line Regions*

3.1.1. *Extinction*

Extinction within the circumnuclear emission-line regions (up to 4″–5″ from the nucleus) was obtained using the observed Hα/Hβ intensity ratio after correction by the extinction in our galaxy [$E(B-V) = 0.028$ mag., Burstein & Heiles 1984] and assuming a case B recombination value.

The extranuclear emission-line regions located well above the plane of the galaxy at projected distances of 20″ (P.A. 55°) and 40″ (P.A. 35°) do not show any indication of a significant amount of interval extinction. On the other hand, an extinction of $E(B-V) = 0.2$ in the regions SW of the nucleus and $E(B-V) = 0.6$ in th regions NE of the nucleus was obtained. Considering the weakness of Hβ and the uncertainty in the Hα flux due to the blending with the strong [N II] emission lines, an uncertainty in the derived extinction of $E(B-V) = \pm0.1$ was estimated.

It has been argued by Halpern & Steiner (1983) that in nebulae ionized by a hard X-ray continuum, as could be true in NGC 4388, collisional excitations could increase the theoretical Hα/Hβ ratio to 3.1 instead of 2.86 as it is in case B recombination. If these collisional effects are considered the extinction values $E(B-V)$ given above would be decreased by $\Delta E(B-V) = 0.07$.

Our results are consistent with previous measurements by PM. These authors reported an extinction of $A_V = 1.0 \pm 0.2$

mag for the nucleus of NGC 4388. Also, the presence of a broad Hα emission line at around 4″ NE of the nucleus detected by Shields & Filippenko (1988) has been interpreted by these authors as a consequence of scattering by dust particles of broad-line region (BLR) photons into our line of sight, although they do not give any value of the minimum amount of dust and extinction required.

3.1.2. Amount of Dust

A rough estimate of the amount of dust present in these circumnuclear regions can be obtained using the detailed three component model (Seyfert, circumnuclear starburst, and disk) of Rowan-Robinson & Crawford (1987) to explain the four IRAS fluxes in NGC 4388. According to these authors the amount of infrared luminosity (log $L_{Seyfert} = 9.49 \, L_\odot$ for a distance of 19.7 Mpc) associated with a spherically symmetric dust distribution directly illuminated by the Seyfert nucleus corresponds to a total dust mass of $M_{dust} = 48 \, M_\odot$. These dust grains would be located at a maximum distance of 23 pc from the nucleus, but if clumps of cold gas and dust are considered its distance would increase by a factor $C^{-0.5}$ where C is the covering factor of the clumps. If on the other hand, we consider the ionizing source radiating within a cone and a spherical distribution of dust particles, there will be some dust not heated by the nucleus and, therefore, the total amount of dust calculated by Rowan-Robinson & Crawford should be considered as a low limit.

3.2. Physical Conditions: Electron Temperature and Density

Values of the electron temperature and density within the emission-line regions have been obtained using the standard [O III] $\lambda\lambda4959 + 5007$ over [O III] $\lambda4363$ and [S II] $\lambda6717$ over [S II] $\lambda6731$ line ratios, respectively (see Aller 1984 for explicit equations). Figure 1 shows the spectrum of the nucleus of NGC 4388 used to measure the relative flux of the [O III] and [S II] emission lines and therefore to derive temperatures and densities. Spectra around the nucleus have similar S/N ratios.

Uncertainties in temperature determinations are largely due to the faintness of the [O III] $\lambda4363$ emission line. An additional problem is that with our spectral resolution (12 Å) this

line is blended with Hγ. Considering all these facts, an electron temperature of $T_e = 15,500 \pm 3000$ K within 3″ around the nucleus is obtained. This temperature represents the mean value of several independent measurements using the various spectra at and around the nucleus and along the three different position angles observed.

For the extranuclear extended emission line regions (EELR) located above the plane of the galaxy, no [O III] $\lambda4363$ emission line was detected, and therefore no temperature was obtained. However, the electron temperature measured in EELR around radio galaxies ranges between 10^4 to 2×10^4 K (Robinson et al. 1987). Therefore, an electron temperature of 1.5×10^4 K will be assumed for the EELR around NGC 4388.

The electron density was calculated using the [S II] emission lines. This gives a mean value of $N_e = 400 \pm 100$ cm^{-3} for the nucleus, that is, the region within the first arcsecond around the emission peak, and a density of $N_e = 200 \pm 100$ cm^{-3} at distances between 2″–4″ from the nucleus.

Finally, density values below the low-density limit for the [S II] lines are obtained for the regions R_{35}^{40} and R_{55}^{20} (located at projected distances of 40″ and 20″ from the nucleus along directions P.A. 35° and 55°, respectively). The density values are lower by a factor of 3 with respect to those obtained from the [S II] line ratios given by Pogge (1988). This discrepancy can be understood as the combined effect of the intrinsic weakness of the lines plus blending caused by low spectral resolution in Pogge's and our data. A density of $N_e = 50$ cm^{-3} is assumed for these extranuclear regions which should be considered most likely as an upper limit.

3.3. Mass and Filling Factor of the Emission-Line Regions

If the electron temperature in the extranuclear emission-line regions is similar to that measured for the circumnuclear gas (see previous subsection), the mass and filling factor of these regions can be obtained as a function of the Hα luminosity:

$$M_g = 4.44 \times 10^{-33} L(H\alpha) N_e^{-1} \, M_\odot \, , \qquad (1)$$

$$f = 1.27 \times 10^{-40} L(H\alpha) N_e^{-2} l^{-1.5} a^{-1.5} \, , \qquad (2)$$

where l an a are the projected dimensions in kiloparsecs and N_e is the electron density as given in § 3.2. The results for the extranuclear regions and the circumnuclear region along the radio emission are presented in Table 2. Lower limits on the
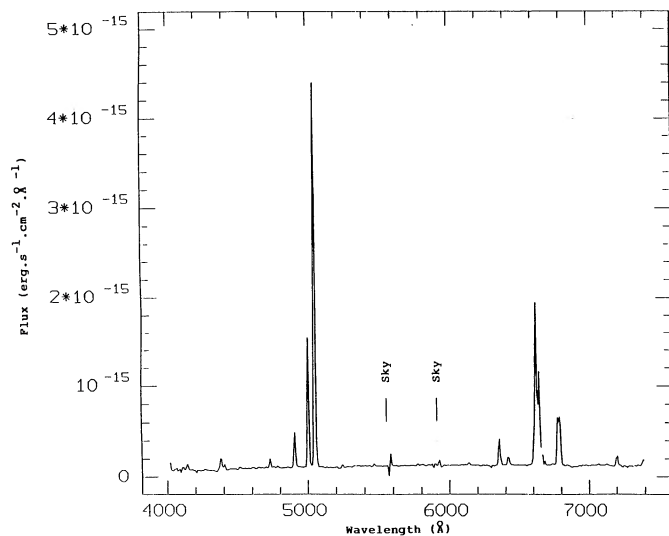

FIG. 1.—Spectrum of the nucleus of NGC 4388 showing all the emission lines over the spectral region 4000–7000 Å.

TABLE 2

PHYSICAL PROPERTIES OF THE EMISSION-LINE REGIONS

Region[a]	R_{23}^4	R_{35}^{40}	R_{55}^{20}
Distance (kpc)[b]	0.38	3.82	1.91
Size (kpc, kpc)[b]	0.55, 0.2	1.15, 0.2	1.15, 0.2
Temperature (K)[c]	15500	15000	15000
Density (cm^{-3})	200	≤ 50	≤ 50
$L(H\alpha)$ (10^{38} ergs s^{-1})	16.4	1.2	0.9
Ionized mass ($10^4 \, M_\odot$)	3.6	≥ 1.0	≥ 0.8
Filling factor (10^{-4})	1.4	≥ 0.6	≥ 0.4
N_{ph}^{ion} (10^{50} photons s^{-1})[d]	12.3	0.9	0.7

[a] Different regions are labeled as $R_{P.A.}^d$ where d means the projected distance to the nucleus in arcseconds and "P.A." means the position angle.

[b] These values are the projected distance to the nucleus and projected size of the emission-line regions, respectively.

[c] See discussion in § 3.2.

[d] These values correspond to a covering factor equal to unity. Therefore, they must be considered as a low limit.

ionized gas masses and filling factors for the extranuclear emission-line regions are of the order of 10^4 $M_\odot$ and in the range 5×10^{-5}–10^{-4}, respectively.

3.4. Excitation Conditions in the Extended Emission-Line Regions

Excitation conditions in the different emission-line regions can be compared and parameterized through the usual ionization parameter $U = N_{ph}^{ion}[4\pi R^2 N_e c]^{-1}$ using the various line ratios as tabulated in Table 3. This table gives the logarithm of the ratios of the strongest emission lines (He II $\lambda 4686$, Hβ, [O III] $\lambda 5007$, [O I] $\lambda 6300$, Hα, [N II] $\lambda 6584$, and [S II] $\lambda\lambda 6717$, 6731) for the different emission-line regions without any internal reddening correction. Also included for comparison are the ratios obtained for shock heating models (Binette, Dopita, & Tuohy 1985), and photoionization models with a nonthermal source (Stasińska 1984), a cluster of stars (Evans & Dopita 1985), or evolutionary models of H II regions with extreme Wolf-Rayet stars (García-Vargas 1991).

From these ratios it is clear that the nucleus, the circumnuclear (labeled as R_{SW}^4 and R_{NE}^4 in Table 3), and the extranuclear emission regions (labeled as R_{55}^{20} and R_{35}^{40} in Table 3) all share similar ionization conditions. These excitation conditions are best characterized by a nonthermal ionizing source with ionization parameter $U \approx 5 \times 10^{-3}$ and power-law ionizing continuum ($F_\nu \propto \nu^{-\alpha}$) with $\alpha = 1.5$ (see also Robinson et al. 1987), although evolutionary models of star clusters with a mass of 4×10^4 $M_\odot$ reproduce the emission-line ratios during certain stages of their evolution (see models H II–3.5E6 in Table 3 and a more detailed discussion in § 4.1.1).

Efforts have also been made to explain the line ratios of the NGC 4388 extended emission regions as produced by a radiation-supported accretion disk around a black hole (Acosta-Pulido et al. 1990). In these models the ionization parameter and the shape of the ionizing continuum are controlled by the mass of the hole and size of the accretion disk. Although promising, none of their best-fitting models give an appropriate account of the observed emission-line ratios, in particular the low-ionization lines. This effect is mostly likely understood as a lack of soft X-ray photons in the predicted accretion disk ionizing continuum.

4. DISCUSSION

As already pointed out in § 3.4, the excitation conditions of the extranuclear extended emission-line regions (R_{35}^{40} and R_{55}^{20} in Table 3) are similar to those measured in the nucleus and circumnuclear regions (R_{23}^4, R_{NE}^4, R_{SW}^4). This fact can easily be considered as evidence for the gas in these regions being ionized by the same ionizing continuum: the central nonthermal source. However, under this hypothesis, if the electron density remains almost constant in the different emission regions (see discussion in § 4.3), one would naively expect a decrease in the ionization parameter proportional to R^{-2} where R is the distance to nucleus. Since we cover a range of projected distances from 0.4 to 4 kpc, a decrease of the ionization parameter by as much as two orders of magnitude would be expected. This is contrary to what is observed.

On the other hand if the electron density decreases as R^{-2}, this will balance the radial dilution of the central continuum source, and we will get a constant ionization parameter as observed. However, since the emission lines are recombination or collisionally excited lines, the emissivity will depend on N_e^2 and the surface brightness would be a factor 10^{-4} fainter in the extranuclear extended emission-line regions than it is in the circumnuclear regions. This expected result is also contrary to what it is measured.

Peculiar situations like this have already been detected in extranuclear emission-line regions around 3C 227 (Fosbury

TABLE 3

EXCITATION INDICATORS OF THE EELR AND NUCLEUS[a]

Region[b]	[O I]/[O III]	[O III]/Hβ	He II/Hβ	[N II]/Hα	[O I]/Hα	[S II]/Hα
Nucleus:	−1.19	1.07	−0.67	−0.24	−0.78	−0.25
R_{NE}^4	−1.13	0.97	...	−0.30	−0.90	−0.27
R_{SW}^4	−1.30	1.06	...	−0.28	−0.78	−0.27
R_{23}^4	−1.03	0.79	...	−0.37	−0.98	−0.35
R_{35}^{40}	...	0.94	...	−0.37	...	−0.22
R_{55}^{20}	...	1.04	...	−0.20	...	−0.34
Shock[c]	−0.88	0.73	...	−0.08	−0.64	0.10
Photon-3[d]	−1.17	0.81	−0.75	−0.16	−0.82	−0.15
Photon-2[d]	−2.39	1.17	−0.79	−0.81	−1.69	−0.77
H II[e]	−1.94	0.12	...	−0.65	−2.28	−1.22
H II–3.5E6[f]	−1.23	0.72	...	−0.25	−0.94	−0.18
H II–4.0E6[f]	−0.93	0.64	...	−0.08	−0.72	0.005

[a] Mean uncertainty of ±0.05 is obtained for the emission-line regions in the nucleus, R_{NE}^4, and R_{SW}^4, while this increases to ±0.09 for the rest of the emission-line regions.

[b] The different regions are labeled as $R_{P.A.}^d$, where d means the projected distance to the nucleus in arcsecond and P.A. means the position angle. When P.A. equals SW and NE, the numbers indicate the mean of the emission-line ratios at P.A. 203, 215, 235, and at P.A. 35 and 55, respectively.

[c] Radiative shock model B53 of Binette et al. 1985 characterized by $V_{shock} = 116$ km s^{-1}, $N_e([S II]) = 270$ cm^{-3}, $T_e([O III]) = 26,900$ K, and solar abundances.

[d] Nonthermal photoionization models from Stasińska 1984 characterized by a spectral index of $\alpha = 1.5$, an ionization parameter of $U = 10^{-3}$ and 10^{-2}, respectively, and solar abundances.

[e] H II region photoionization model from Evans & Dopita 1985 characterized by an ionization parameter of $U = 3 \times 10^{-3}$, an ionizing temperature $T_{ion} = 4 \times 10^4$ K, and solar abundances.

[f] Evolutionary H II region models with post–main-sequence stars from García-Vargas 1991. This model is characterized by a total mass of 4×10^4 $M_\odot$, an initial mass function with slope $\alpha = 2.35$, a mass range between 0.85 and 120 $M_\odot$, size of 250 pc, an electron density of 10 cm^{-3}, and an ionization parameter of log $U = -2.94$. Models correspond to a star cluster at 3.5 and 4.0×10^6 yr after the initial burst.

1989) and IC 5063 (Colina et al. 1991). Fosbury found the brightest extranuclear emission-line regions to also be those with the highest ionization parameter, while Colina et al. (1991) measured a radial decrease in the surface brightness of Hα and [O III] incompatible with the observed behavior of the ionization parameter.

In the following sections several alternatives related to the presence of local ionizing sources and/or changes in the structure of the emitting gas are explored in order to understand these results.

4.1. Ionizing Source

4.1.1. Local Ionizing Star Cluster

The total number of ionizing photons needed to explain the Hα luminosity measured in the extranuclear emission-line regions can be given by the expression

$$N_{ph} = 7.52 \times 10^{11} L(H\alpha)\Omega^{-1} \text{ photons s}^{-1} \qquad (3)$$

if an electron temperature of 15,000 K is assumed. In this expression Ω represents the covering factor of the gas clouds with respect to the ionizing source.

If one considers (1) a Salpeter law with $\alpha = 2.35$, (2) a stellar mass range from 0.1 to 100 $M_\odot$, (3) the mean ionizing luminosity of an O-type star equal to 10^{49} photons s^{-1} (see Mezger, Smith, & Churchwell 1974; Osterbrock 1989), and (4) that the total amount of ionizing photons comes from massive main-sequence stars ($M \geq 20\ M_\odot$), the total number of stars and mass needed to explain the total ionizing photons given by expression (3) is

$$N_*^T = 7.52 \times 10^{-38} L(H\alpha)\Omega^{-1} \frac{\int_{0.1 M_\odot}^{100 M_\odot} m^{-\alpha}\, dm}{\int_{20 M_\odot}^{100 M_\odot} m^{-\alpha}\, dm}, \qquad (4)$$

$$M_*^T = 7.52 \times 10^{-38} L(H\alpha)\Omega^{-1} \frac{\int_{0.1 M_\odot}^{100 M_\odot} m^{-\alpha+1}\, dm}{\int_{20 M_\odot}^{100 M_\odot} m^{-\alpha}\, dm}. \qquad (5)$$

Under the hypothesis of a local cluster of ionizing stars, the covering factor will be nearly 1 ($\Omega \leq 1$). Considering the total Hα luminosity measured in these regions (see Table 2), a total number of ionizing photons $N_{ph} \geq 10^{50}$ photons s^{-1} is obtained from expression (3). This corresponds to a total number of stars $N_*^T \geq 14{,}400$ and a total mass of $M_*^T \geq 5100$ $M_\odot$. Such a cluster would be very difficult to detect unless deep CCD images are used.

Therefore, based solely on luminosity arguments, a low-mass star cluster with massive main-sequence stars would be a reasonable local source of ionization. However, the emission-line ratios (see Table 3), do not agree with those expected from ionization by hot stars (Evans & Dopita 1985; Veilleux & Osterbrock 1987). Even detailed evolutionary H II region models (García-Vargas 1991) with luminous post–main-sequence stars like extreme Wolf-Rayet stars are unable to reproduce the observed emission-line ratios over long periods of time. They only reproduce the detected emission-line ratios during a short time interval of less than 5×10^5 yr after 3.5×10^6 yr since the starburst began (see Table 3). The presence of high-excitation extranuclear emission-line regions is a typical phenomenon among Seyferts and high-luminosity radio galaxies; consequently a hard ionizing continuum lasting for longer periods of time is most likely needed to get the overall high-excitation conditions in NGC 4388 and in its associated extended emission regions.

4.1.2. Ionization Due to Relativistic Particles and Shocks Associated with the Radio Emission

There have been some suggestions that relativistic electrons associated with radio synchrotron emission could play an important role in the heating and ionization of gaseous nebulae if the relativistic and thermal plasma coexist (Ferland & Mushotzky 1984).

If photons and relativistic electrons are considered as ionizing sources, the relative importance of the electrons with respect to the photons is given by the expression (Wilson et al. 1988)

$$\frac{\Gamma_e}{\Gamma_{ph}} = \frac{10^{-8}}{U} \frac{P_e}{P_{th}}, \qquad (6)$$

where U is the usual ionization parameter due to nonthermal ionizing radiation and P_e and P_{th} are the pressures corresponding to relativistic and thermal electron density, respectively. Consequently, for an ionization parameter $U \approx 5 \times 10^{-3}$ and assuming that relativistic and thermal electron pressures are of the same order (Unger et al. 1986), a ratio $\Gamma_e/\Gamma_{th} \approx 2 \times 10^{-5}$ is obtained. Therefore, it is very unlikely that the ionizing effect of relativistic electrons could play a major role in the excitation of the emission-line regions in general and for NGC 4388 in particular.

Another alternative related to the radio-emitting plasma is the presence of radiative shocks as a consequence of the motion of the radio plasma/jet within the dense interstellar medium. This mechanism requires that both radio emission and line-emitting gas are spatially coincident or, at least, located along the same orientation. In NGC 4388 this requirement can only be valid along position angle P.A. 20°–25°, where recent 20 and 6 cm VLA radio maps (Stone et al. 1988; Saikia & Hummel 1989) show the presence of an elongated radio emission tongue which deviates to the north at larger distances.

If radiative shocks are present in these regions, we would expect an emission-line spectrum characterized by low-ionization emission lines stronger relative to high ionization emission lines than if the nebulae were ionized by a hard nonthermal source. Although we measure a decrease in the [O III]/ Hβ ratio for R_{23}^4 (see Table 3) that could be compatible with radiative shocks, all the other low-ionization emission lines are weaker than otherwise expected in radiative shocks (see Table 3 and Binette et al. 1985). So, it is concluded that radio emission is, if anything, a minor source of ionization for the emission-line regions associated with NGC 4388. However, recent shock plus photoionization composite models can fit the observed emission line ratios in Seyfert 2 galaxies under certain conditions (Viegas-Aldrovandi & Contini 1989).

4.1.3. Central Nonthermal Ionizing Source

Although any of the previous ionization sources could help to maintain the excitation conditions in the observed EELR, none of them can be considered as the main ionizing source. There is however, one source, the central nonthermal source, that gives the appropriate ionizing luminosity and has sufficient energy to explain the high-excitation conditions throughout.

Using the IUE spectrum SWP 23104 from the VILSPA-IUE data bank, a spectral index $\alpha = 0.43$ ($F_\nu = k\nu^{-\alpha}$) was measured in the 1200–2000 range. Also a continuum flux of $F_\lambda(1500$ Å$) = 5.04 \times 10^{-15}$ ergs s^{-1} Å^{-1} cm^{-2} was obtained after cor-

recting for an extinction $E(B-V) = 0.028$ due to our own galaxy (Burstein & Heiles 1984).

For an ionizing power-law spectrum, the total number of ionizing photons along our line of sight is given by

$$N_{\text{LOS}}^{\text{ion}} \approx D^2 F_\nu(912 \text{ Å})[h\alpha]^{-1}, \qquad (7)$$

where $D = 19.7$ Mpc, $\alpha = 0.43$, $F_\nu(912 \text{ Å}) = 3.05 \times 10^{-27}$ ergs $s^{-1} \text{ cm}^{-2} \text{ Hz}^{-1}$, h represents Planck's constant and no internal reddening was considered. One gets $N_{\text{LOS}}^{\text{ion}} = 3.96 \times 10^{51}$ photons $s^{-1} \text{ sr}^{-1}$ or $N_{\text{ph}}^{\text{ion}} = 4\pi N_{\text{LOS}}^{\text{ion}} = 4.98 \times 10^{52}$ protons s^{-1} if the radiation source is isotropic and radiates in all directions the same flux as we observe along our line of sight.

This is powerful enough to ionize the extranuclear emission-line regions. Since the photons needed to ionize these regions were $N_{\text{ph}} \approx 7.5 \times 10^{49} \, \Omega^{-1}$ (see expression [3] and Table 2), a covering factor of $\Omega \leq 1.5 \times 10^{-3}$ is obtained. This is a typical value for the extended emission-line regions around active galaxies (Robinson et al. 1987).

Based on ionizing luminosities and emission-line ratios arguments (see § 3.4,), the central non-thermal source is the most likely mechanism capable of explaining the existence of the high-excitation extranuclear emission-line regions around NGC 4388. However, it still has a problem, mainly that the ionization parameter should have an R^{-2} radial dependence if the electron density remains constant over all the regions, or that the emission-line surface brightness of the extranuclear regions should be 10^4 times fainter than that around the nucleus if the density decreases with distance, or 10^3 times fainter if also an increase in column depth at large distances is included (see § 4.3 for further discussion).

4.2. Hidden Luminous Seyfert 1 Nucleus

There is observational evidence suggesting that NGC 4388 has a hidden luminous Seyfert 1 nucleus. Shields & Filippenko (1988) detected a broad Hα component off the nucleus. They suggest that this is produced by dust obscuring our vision of the nucleus and scattering BLR photons into our line of sight. Probably the best evidence suggesting the presence of a luminous nonthermal nucleus at the center of NGC 4388 comes from the recent detection of NGC 4388 as the brightest Virgo cluster source in the range 2–10 keV (Hanson et al. 1990). These authors measured a luminosity of log L_x(2–10 keV) = 42.0 ergs s^{-1} that places NGC 4388 among the Seyfert 1 galaxies.

In addition, high-resolution 4.86 GHz VLA maps (FWHM = $0''.4$: Saikia & Hummel 1989) show the presence of two radio emission peaks located (as measured directly from the Saikia and Hummel radio map) at positions $\alpha_A = 12^h23^m14^s.64$, $\delta_A = 12°56'20''.0$ and $\alpha_B = 12^h23^m14^s.59$, $\delta_B = 12°56'18''.2$ separated by $2''$ along position angle P.A. 21°. These two peaks are also displaced from the optical nucleus $\alpha_{\text{opt}} = 12^h23^m14^s.56$, $\delta_{\text{opt}} = 12°56'17''.35$ (R. W. Argyle private communication quoted in Stone et al. 1988). Finally the IRAS emission peak is located at position $\alpha_{IRAS} = 12^h23^m14^s.4$, $\delta_{IRAS} = 12°56'23''$ as listed in the IRAS Point Source Catalog. Within the IRAS position uncertainties (ellipse with semiaxis $30'' \times 6''$ at position angle 113°: Fullmer & Lonsdale 1989), these measurements marginally suggest that the true nucleus corresponds to peak A in the high-resolution VLA radio map.

In the following, the flux of the coronal [Fe VII] λ6087 emission line and the UV and IRAS luminosity are used to strengthen the idea that the ionizing source in NGC 4388 is a central luminous hidden Seyfert 1 nucleus.
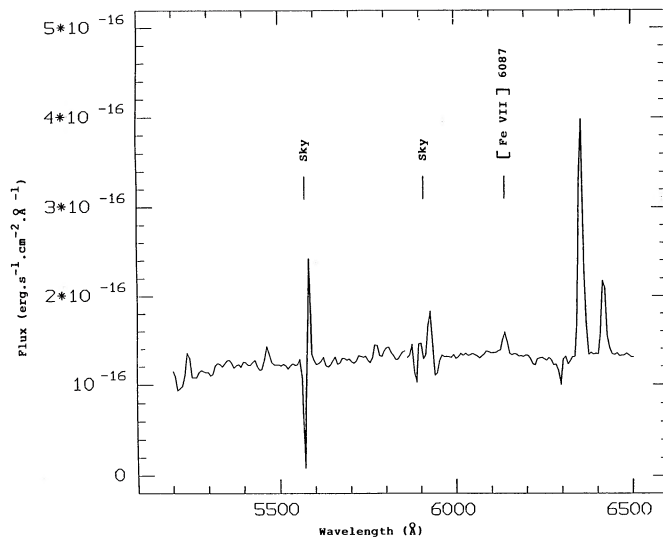

FIG. 2.—Detail of the previous spectrum showing the presence (indicated by an arrow) of the [Fe VII] λ6087 emission line.

4.2.1. Coronal Emission Lines

As shown in the spectrum of the nucleus of NGC 4388 (see Fig. 2), the [Fe VII] λ6087 emission line is detected as in many other Seyfert 2 galaxies (see Koski 1978; Morris & Ward 1988). This line is only observed within $2''$ of the nucleus and its luminosity is interpreted as evidence for the presence of dense clouds of gas, and for the existence of a local and hard extreme UV ionizing source (ionization potential of Fe^{6+} corresponds to 100 eV).

When the dereddened [Fe VII] λ3760/[Fe VII] λ6087 ratio is available in Seyfert 2 galaxies (Koski 1978), it has a value close to one. This value is consistent with electron densities and temperatures of 10^7 cm^{-3} and 2–3×10^4 K, respectively (see Nussbaumer & Storey 1982). Moreover, Díaz and collaborators (Díaz, Prieto, & Wamsteker 1988) have measured, using the [Ne IV] λ2424 and [Ne IV] λ4726 lines, a density of $\approx 3 \times 10^5 \text{ cm}^{-3}$ for the regions emitting the high-ionization [Ne IV] lines (ionization potential $Ne^{3+} = 63.5$ eV) in the Seyfert 2 galaxy NGC 3393.

Penston and collaborators (Penston et al. 1984) concluded that the existence of coronal lines like [Fe VII] λ6087 in the spectra of Seyfert galaxies is most likely due to a photoionization process. Collisional ionizations working in high-temperature plasmas were considered not relevant in the nucleus of active galaxies. An estimate of the number of ionizing photons with energies greater than 100 eV can be obtained under the assumption of photoionization, and considering that the Fe^{6+} and He^{++}–emitting regions would most likely be the same or, at least, that the [Fe VII] λ6087 photons would be generated in the inner front of the He^{++}–emitting region. This hypothesis is supported by the similarity of the He II λ4686 and [Fe VII] λ6087 emission-line profiles observed in some Seyfert galaxies like Mrk 359 and NGC 4151 (Veilleux 1991). Therefore,

$$N_{\text{ph}}(\geq 100 \text{ eV}) \approx V(Fe^{6+})N(He^{++})N_e \alpha_B(He^+). \qquad (8)$$

Here, the volume $V(Fe^{6+})$ is giving as $V(Fe^{6+}) = L([\text{Fe VII}] \lambda 6087)/\epsilon([\text{Fe VII}] \lambda 6087)$ where $\epsilon([\text{Fe VII}] \lambda 6087)$ is the emissivity of the line. It has the expression $\epsilon([\text{Fe VII}] \lambda 6087) = N(Fe^{6+}, {}^1D_2)A({}^1D_2)h\nu_{6087}$, where $N(Fe^{6+}, {}^1D_2)$ is

the upper-level population and $A(^1D_2)$ is the radiative transition probability.

Assuming that the [He^{++}/Fe^{6+}] abundance ratio is equal to the solar [He/Fe] abundance, one obtains

$$N_{ph}(\geq 100 \text{ eV}) \approx 1.61$$
$$\times 10^{15} L([\text{Fe VII}] \ \lambda 6087) N_e \alpha_B(\text{He}^+)[N(^1D)]^{-1} \quad (9)$$

where $\alpha_B(\text{He}^+) = 1.2 \times 10^{-12}$ cm^3 s^{-1}, $N(^1D) = N(\text{Fe}^{6+} \ ^1D_2)/N(\text{Fe}^{6+}) = 1.14 \times 10^{-2}$ (Nussbaumer & Storey 1982) for $T_e(\text{Fe}^{6+}) = 15,000$ K and $N_e = 10^7$ cm^{-3}. Here $L([\text{Fe VII}] \ \lambda 6087)$ is the [Fe VII] $\lambda 6087$ luminosity after correction of the extinction within our galaxy and is equal to 1.1×10^{38} ergs s^{-1}. Therefore, the total number of photons with energies greater than 100 eV will be $N_{ph}(\geq 100 \text{ eV}) \approx 2 \times 10^{50}$ ph s^{-1} or larger if internal extinction is present.

A rough estimate of the luminosity in the EUV–soft X-ray energy range is obtained if one considers a mean energy of 250 eV per photon in that range. Therefore, log $L(\text{EUV–soft X}) \gtrsim 40.8$ ergs s^{-1} which lies in between the measured X-ray luminosities log $L_X(0.5–3.0$ keV) $= 40.23$ ergs s^{-1} (Forman et al. 1979) and log $L_X(2–10$ keV) $= 42.0$ ergs s^{-1} recently obtained by Hanson and collaborators (Hanson et al. 1990).

4.2.2. *Ionizing vs. Far-Infrared Luminosities*

If one assumes that a fraction of the total infrared luminosity detected in NGC 4388 comes from dust-reprocessed UV and X-ray radiation, one would expect that this infrared luminosity would be a fraction of the total ionizing luminosity depending on the covering factor of the dust distribution located around the nucleus.

For NGC 4388, a three-component (Seyfert, starburst, and disk) dust model has been used to fit the observed *IRAS* fluxes (Rowan-Robinson & Crawford 1989). These authors give a total infrared luminosity radiated by warm dust directly heated by the Seyfert nucleus equal to log $L_{FIR}^{Seyfert} = 43.07$ ergs s^{-1} when scaled to a distance of 19.7 Mpc. On the other hand, if one considers a mean energy of 35 eV for the nonthermal ionizing photons and a total number of ionizing photons as if the source was radiating isotropically with a UV flux equal to the one measured along our line of sight and without any internal obscuration, that is, $N_{ph}^{ion} = 4.98 \times 10^{52}$ photons s^{-1} (see § 3.3), a total UV–extrapolated ionizing luminosity log $L_{UV} = 42.45$ ergs s^{-1} is obtained.

For NGC 4388 the measured opening angle of the ionizing cone defined by the extranuclear emission-line regions is $2\theta \approx 60°$, corresponding to one-third of the 4π solid angle. If one considers that the ionizing cone is free of dust, that the dust distribution around the nucleus has a planar or toroidal morphology coincident with the galaxy's plane, and that the ionizing source radiates isotropically with a flux equal to the cone measured along our line of sight, one would expect $L_{FIR}^{Seyfert} \approx 0.7 L_{UV}$. On the contrary we find $L_{FIR}^{Seyfert} = 4.2 L_{UV}$.

To bring these two results together, a central source which is around 6 times brighter in the ionizing energy range than otherwise detected is required. This implies an extinction in the nucleus (distances shorter than 100 pc) of at least $A_V \approx 0.31$ and indicates that the UV-extrapolated ionizing luminosity of NGC 4388 should be log $L_{UV} \approx 43.23$ ergs s^{-1}, placing it among intermediate luminosity Seyfert 1 galaxies.

Finally, one should bear in mind that the way in which the ionizing luminosity is derived depends strongly on the spectral index of the power law. If one considers that the spectral index

$\alpha = 0.43$ measured in the UV region is valid over the whole spectral region 3000 Å–1 keV, then the total number of ionizing photons available for dust heating should be increased by a factor of 2. On the other hand, if one assumes a spectral index $\alpha = 1.0$ (unified Seyfert 1 continuum slope over the X-ray–IR spectral range: Carleton et al. 1985), the total ionizing luminosity will drop by a factor of around 1.5. Therefore, the consequence of a flat or steep spectral index will be the decrease or increase in the obtained obscuration of the central nonthermal source. It is therefore important to have simultaneous spectral coverage in individual galaxies like NGC 4388 to further check the obscuration hypothesis using the luminosity arguments.

4.3. *Substructure of the Emission-Line Regions: Two Phase Medium?*

So far it was found that for an electron density of $N_e = 50$ cm^{-3} (see § 3.2), the total ionized gas mass in the extranuclear emission-line regions was of the order of $10^4 \ M_\odot$, with corresponding filling and covering factors of the order of 5×10^{-5} and 1.5×10^{-3}, respectively. These parameters suggest that the extranuclear emission-line regions have a clumpy structure formed by sheets, filaments, or small clouds of gas with sizes of the order of parsecs.

However, the derived mass and filling factor are a strong function of the electron density (see expressions [1] and [2] in § 3.3). Therefore if the mean electron density in the extranuclear emission-line regions is dropped to a value of $N_e = 1$ cm^{-3}, as Hβ surface brightness in radio galaxies suggest (Tadhunter 1987), the ionized mass and filling factor would increase by factors 50 and 2500, respectively. Under this assumption, the structure of the extranuclear emission-line regions would be that of a diffuse cloud of ionized gas, size around 1 kpc, occupying a large fraction ($\approx 10\%$) of the projected volume.

In this case, the extended emission-line regions will most probably consist of a two-phase medium in equilibrium small dense clumps of gas immersed in a more diffuse hotter medium.

If the small dense and warm clumps of gas are not confined, they will disintegrate in time scales similar to those needed by a sound wave to travel a distance similar to the radius of the clump, that is,

$$t_{expand} = r_c/v_s \approx 8.2 \times 10^4 r_c \ T_4^{-0.5} \text{ yr}, \quad (10)$$

where r_c represents the radius of the clump in parsecs and T_4 the electron temperature of the clump in units of 10^4 K. If an electron temperature of $T_4 = 1.5$ and a radius $r_c \approx 5$ pc are assumed (recent *HST* images of the circumnuclear regions of NGC 1068 show individual emission-line regions resolved with sizes of 10 pc; Evans et al. 1991), typical time scales of $t_{expand} \approx 3 \times 10^5$ yr are obtained. Since extended extranuclear emission-line regions are very common around Seyfert and radio galaxies (Baum et al. 1988), it is very unlikely that the existence of these regions is a short and transient phenomenon unless we can imagine a mechanism capable of creating clumps of gas at such distances from the center of the galaxies and at a similar rate as they evaporate. Therefore, these clumps would most likely be confined by an external medium.

If it is assumed that NGC 4388 lies near the center of the Virgo cluster (see PM for a discussion), we could consider that the extranuclear emission-line regions above the disk of NGC 4388 are immersed in the hot X-ray–emitting gas observed at the core of the Virgo cluster. Forman et al. (1979) measured an electron density of $N_e^{ICM} = 5 \times 10^{-4}$ cm^{-3} and an

electron temperature of $T_e^{\mathrm{ICM}} = 1.2 \times 10^8$ K for the X-ray–emitting intracluster medium in Virgo.

If the radiative losses of the line–emitting clouds balance the heating due to the ionizing source and to conduction, these small clumps could coexist in pressure equilibrium with low-density hot gas (see McCray 1987).

On the other hand, if radiative losses do not compensate the heating, the evaporation time of these small clumps of gas immersed in a very hot external gas due to thermal conduction would be very short. According to Cowie & McKee (1977), the evaporation time would be given by the expression

$$t_{\mathrm{evap}} = 1044 r_c^2 N_e T_7^{-2.5} \text{ yr} , \qquad (11)$$

when radiative losses are unimportant. In this expression r_c represents the radius of the clump, N_e the electron density of the clump, and T_7 the temperature of the external gas in units of 10^7 K. For $r_c \approx 5$ pc, $N_e \approx 50$ cm^{-3}, and $T_7 = 12$, the evaporation time corresponds to $t_{\mathrm{evap}} \approx 3 \times 10^3$ yr.

Therefore, if cooling does not balance heating, these dense clouds of gas could not survive direct contact with an X-ray–emitting gas for long time. In this last case, a speculative alternative could be suggested in the form of a two-phase medium: dense clumps immersed in a more diffuse and warmer medium, both heated by the same ionizing source and the last in direct contact with the intracluster medium. The clumps would be characterized by an electron density of $N_e \approx 50$ cm^{-3}, an electron temperature of $T_e \approx 1.5 \times 10^4$ K, and a radius of $r_c \approx 5$ pc, while the diffuse medium would have $N_e \approx 1$ cm^{-3}, $T_e \approx 5 \times 10^5$ K, and a typical size of around 1 kpc. These two media would be in pressure equilibrium. However, one should bear in mind that gas at temperatures of around 10^5 K is thermally unstable (Krolik, McKee, & Tarter 1981; McCray 1987).

High-resolution X-ray observations together with a reliable determination of the electron density and temperature in the extranuclear emission-line regions are needed to further discuss and investigate this two-phase medium hypothesis.

5. SUMMARY

New spectroscopic observations of the extended emission-line regions around NGC 4388 together with archived *IUE*, and published *IRAS*, results have been presented. The following conclusions can be drawn:

1. Based on the luminosity of the [Fe VII] $\lambda6087$ emission line and on the comparison between the far-infrared luminosity and the UV-extrapolated ionizing luminosity as measured along our line of sight, it is concluded that NGC 4388 has a hidden hard ionizing luminous nucleus obscured by at least $A_V = 0.31$ mag. This ionizing source is characterized by $N_{\mathrm{ph}}(\geq 100 \text{ eV}) \gtrsim 2 \times 10^{50}$ photons s^{-1} and by an intrinsic UV luminosity around 6 times brighter than otherwise observed (log $L_{\mathrm{UV}} = 42.45$ ergs s^{-1}). This confirms the suggestion by Shields & Filippenko (1988) that NGC 4388 has a hidden luminous Seyfert 1 nucleus.

2. The detection of [Fe VII] lines in emission suggest the presence of high density clouds of gas with electron densities of the order of 10^7 cm^{-3}.

3. Based on line luminosities and emission-line ratios, the extended emission-line regions are ionized by a power-law nonthermal source located at the nucleus of NGC 4388. Alternative ionizing sources considering a cluster of hot stars, relativistic particle, or radiative shocks with the radio emission play a minor role, if any. Current models of ionization by the continuum of a thick accretion disk have problems in explaining the strength of the low-ionization lines. Models of star clusters with evolved post–main-sequence stars are able to reproduce the observed emission-line ratios during very short time scales of the order of 5×10^5 yr.

Overall NGC 4388, is, together with NGC 1068 (Pogge 1988), NGC 4151 (Pérez et al. 1989), NGC 5252 (Tadhunter & Tsvetanov 1989), and IC 5063 (Colina et al. 1991), one of the best candidates to study in detail the issue of anisotropic radiation, obscured nuclei in Seyfert galaxies, and the substructure of the emission-line regions.

REFERENCES

Acosta-Pulido, J., Pérez-Fournon, I., Calvani, M., & Wilson, A. S. 1990, ApJ, 365, 119
Aller, L. H. 1984, Physics of Thermal Gaseous Nebulae, Astrophysics & Space Science Library, Vol. 112 (Dordrecht: Reidel)
Antonucci, R. R. J., & Miller, J. S. 1985, ApJ, 297, 621
Barthel, P. D. 1989, ApJ, 336, 606
Baum, S. A., Heckman, T. M., Bridle, A., van Breugel, W., & Miley, G. 1988, ApJS, 68, 643
Binette, L., Dopita, M. A., & Tuohy, I. R. 1985, ApJ, 297, 476
Browne, I. W. A. 1989, ESO Conf. & Workshop Proc. 32, ESO Workshop on Extranuclear Activity in Galaxies, ed. E. J. A. Meurs & R. A. E. Fosbury (Munich: ESO) 379
Burstein, D., & Heiles, C. 1984, ApJS, 54, 33
Carleton, W. P., Elvis, M., Fabbiano, G., Willner, S. P., Lawrence, A., & Ward, M. 1987, ApJ, 318, 595
Chambers, K. C., Miley, G. K., & van Bruegel, W. 1987, Nature, 329, 604
Colina, L., Fricke, K. J., Kollatschny, W., & Perryman, M. A. C. 1987, A&A, 186, 39
Colina, L., Sparks, W., & Macchetto, F. D. 1991, ApJ, 370, 102
Corbin, M. R., Baldwin, J. A., & Wilson, A. S. 1988, ApJ, 334, 584
Cowie, L. L., & McKee, C. F. 1977, ApJ, 211, 135
Díaz, A. L., Prieto, A., & Wamsteker, W. 1988, A&A, 195, 53

Evans, I. N., & Dopita, M. A. 1985, ApJS, 58, 125
Evans, I. N. Ford, H. C., Kinney, A. L., Antonucci, R. R. J., Armus, L., & Caganoff, S. 1991, ApJ, 369, L27
Ferland, G. J., & Mushotzky, R. F. 1984, ApJ, 286, 42
Ferland, G. J., & Osterbrock, D. E. 1986, ApJ, 300, 658
Filippenko, A. V., & Sargent, W. L. W. 1985, ApJS, 57, 503
Forman, W., Schwarz, J., Jones, D., Liller, W., & Fabian, A. C. 1979, ApJ, 234, L27
Fosbury, R. A. E. 1989, ESO Conf. & Workshop Proc. 32, ESO Workshop on Extranuclear Activity in Galaxies, ed. E. J. A. Meurs & R. A. E. Fosbury (Munich: ESO), 169
Fullmer, L., & Lonsdale, C. 1989, Cataloged Galaxies and QSO Observed in the *IRAS* Survey, Version 2 (Pasadena: Jet Propulsion Laboratory)
García-Vargas, M. 1991, Ph.D. thesis, Univ. Autónoma, Madrid
Halpern, J. P., & Steiner, J. E. 1983, ApJ, 269, L37
Hanson, C. G., Skinner, G. K., Eyles, C. J., & Willmore, A. P. 1990, MNRAS, 242, 262
Heckman, T. M., van Breugel, W., Miley, G. K., & Butcher, H. R. 1983, AJ, 88, 1077
Hummel, E., van Gorkom, J. H., & Kotanyi, C. G. 1983, ApJ, 267, L5
Koski, A. T. 1978, ApJ, 223, 56
Krolik, J. H., McKee, C. F., & Tarter, C. B. 1981, ApJ, 249, 422

Macchetto, F. D., Colina, L., Golombek, D., Perryman, M. A. C., & di Serego Alighieri, S. 1990, ApJ, 356, 389
Madau, P. 1988, ApJ, 327, 116
McCarthy, P. J., van Bruegel, W., Spinrad, H., & Djorgovski, S. 1987, ApJ, 321, L29
McCray, R. 1987, Spectroscopy of Astrophysical Plasmas ed. A. Dalgarno & D. Layzer (Cambridge: Cambridge Univ. Press), 264
Mezger, P. G., Smith, L. F., & Churchwell, E. 1974, A&A, 32, 269
Morris, S. L., & Ward, M. J. 1988, MNRAS, 230, 639
Netzer, H. 1985, MNRAS, 216, 63
Nussbaumer, H., & Storey, P. J. 1982, A&A, 113, 21
Osterbrock, D. E. 1989, Astrophysics of Gaseous Nebulae and Active Galactic Nuclei (Mill Valley: University Science Books)
Penston, M. V., Fosbury, R. A. E., Boksenberg, A., Ward, M. J., & Wilson, A. S. 1984, MNRAS, 208, 347
Pérez, E., Gonzalez-Delgado, R., Tadhunter, C., & Tszetanov, Z. 1989, MNRAS, 241, 31P
Pérez-Fournon, I., & Wilson, A. 1990, ApJ, 356, 456
Phillips, M. M., & Malin, D. F. 1982, MNRAS, 199, 905 (PM)
Pogge, R. W. 1988, ApJ, 332, 702
Robinson, A., Binette, L., Fosbury, R. A. E., & Tadhunter, C. N. 1987, MNRAS, 227, 97

Rowan-Robinson, M., & Crawford, J. 1989, MNRAS, 238, 523
Saikia, D. J., & Hummel, E. 1989, ESO Conf. & Workshop Proc. 32, ESO Workshop on Extranuclear Activity in Galaxies ed. E. J. A. Meurs & R. A. E. Fosbury (Munich: ESO), 165
Sandage, A., & Tamman, G. A. 1984, Nature, 307, 326
Shields, J. C., & Filippenko, A. V. 1988, ApJ, 332, L55
Stasińska, G. 1984, A&AS, 55, 15
Stone, J. L., Wilson, A. S., & Ward, M. J. 1988, ApJ, 330, 105
Tadhunter, C. N. 1987, Ph.D. thesis, Univ. Sussex
Tadhunter, C. N., & Tsvetanov, Z. 1989, Nature, 341, 422
Unger, S. W., Pedlar, A., Axon, D. J., Whittle, M., Meurs, E. J. A., & Ward, M. 1987, MNRAS, 228, 671
Unger, S. W., Pedlar, A., Booler, R. V., & Harrison, B. A. 1986, MNRAS, 219, 387
Veilleux, S. 1991, ApJS, 75, 357
Veilleux, S., & Osterbrock, D. E. 1987, ApJS, 63, 295
Viegas-Aldrovandi, S. M., & Contini, M. 1989, ApJ, 339, 689
Wilson, A. S., & Baldwin, J. A. 1989, AJ, 98, 2056
Wilson, A. S., Ward, M. J., & Haniff, C. A. 1988, ApJ, 334, 121